



A flatness-based nonlinear predictive approach for crane control

Thomas Devos, Jean Lévine

► To cite this version:

Thomas Devos, Jean Lévine. A flatness-based nonlinear predictive approach for crane control. IFAC Workshop on Nonlinear Model Predictive Control for Fast Systems, Oct 2006, Grenoble, France. hal-00575665

HAL Id: hal-00575665

<https://hal-mines-paristech.archives-ouvertes.fr/hal-00575665>

Submitted on 10 Mar 2011

HAL is a multi-disciplinary open access archive for the deposit and dissemination of scientific research documents, whether they are published or not. The documents may come from teaching and research institutions in France or abroad, or from public or private research centers.

L'archive ouverte pluridisciplinaire **HAL**, est destinée au dépôt et à la diffusion de documents scientifiques de niveau recherche, publiés ou non, émanant des établissements d'enseignement et de recherche français ou étrangers, des laboratoires publics ou privés.

A FLATNESS-BASED NONLINEAR PREDICTIVE APPROACH FOR CRANE CONTROL

Thomas Devos* Jean Lévine*

* *Centre Automatique et Systèmes*
35 Rue Saint Honoré, 77300 Fontainebleau, France

thomas.devos@ensmp.fr, jean.levine@ensmp.fr

Abstract: We study in this paper a flatness-based nonlinear predictive control law for a reduced size model of a crane studied in (Kiss, 2001; Kiss *et al.*, 1999; Kiss *et al.*, 2000a; Kiss *et al.*, 2000b).

The controller is composed of two parts: the first one is a traditional PD output feedback to track the reference trajectory and reject small perturbations, the second one consists of updating the reference trajectory from the current estimated state of the crane to the desired equilibrium point on a receding horizon each time the pursuit error exceeds a given threshold.

Simulations are presented to illustrate its performances.

Keywords: nonlinear predictive control, differential flatness, motion planning, crane control.

1. INTRODUCTION

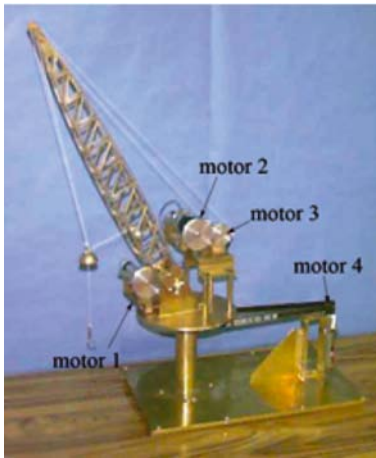


Fig. 1. Reduced size model of the US Navy crane

Cranes are used in various industries such as construction and naval transport. Any automatic control improvement of the assistance to crane

operators may result in an increase of productivity and security.

During operations, the crane is supposed to move as fast as possible to carry the load from an initial position to a desired final destination, avoiding obstacles and sway. Controlling the position of the load requires both motion planning and feedback control to attenuate the perturbations. To this aim, the mechanical degrees of freedom of the crane are actuated, all but those corresponding to the load. In addition, sensors measuring the respective actuators' positions together with two synchronized digital cameras giving the three coordinates of the load via image processing, at a slower but sufficiently high rate, are available. Note that the whole state of the crane model is not directly available through these measurements and must be estimated.

According to the nature of this weight handling system, the presence of large perturbations such as those created by frictions of the motors or belt

elasticity (a belt being used to transmit the motor rotation to the platform) or unknown load mass, and limitations on the motors, make the tuning tradeoff between performance and robustness delicate: to stabilize the load at a rest point, small gains are preferred to keep a good observability of the load oscillations through the motor sensors, whereas to follow fast trajectories, large gains are required. Moreover, if large errors appear, the actuators are soon saturated.

To circumvent this difficulty, we propose a predictive control approach (for recent surveys on this topic see e.g. (Morari and Lee, 1999; Qin and Badwell, 2000)): in addition to a first PD output feedback loop for reference trajectory tracking, each time the pursuit error exceeds a given threshold, the reference trajectory is updated from the (estimated) present state to the desired rest point on a receding horizon. Thus, since we start anew with a reference trajectory at the present estimated state, the tracking error is instantaneously reduced to the estimation error. With this approach, we expect that the rate of decrease of the tracking error is much faster than with pure feedback and certainty equivalence.

This nonlinear predictive control method makes an extensive use of the differential flatness property of the system (see other related linear and nonlinear flatness-based approaches in (Fliess and Marquez, 2000; Delaleau and Hagenmeyer, 2006)) to generate such reference trajectories and stabilize the load along them. It also depends on the observer design used to estimate the tracking error.

The remaining part of the paper is organized as follows. The next section gives a description of our crane reduced size model. In section 3, we present the crane model in three dimensions. The differential flatness of the model and its consequences on motion planning are studied in section 4. We describe in section 5 the basic PD controller used as a first step towards stabilization and perturbation rejection. In section 6, we design an observer estimating the successive derivatives of the flat output and the performances of the observer are studied in simulations. Then the overall predictive control algorithm is presented and simulations showing its efficiency to reduce the oscillations of the load are given in section 7.

2. DESCRIPTION OF THE REDUCED SIZE MODEL OF THE CRANE

The considered model is the reproduction of a US Navy crane at the scale 1/80 (Fig. 1 and 2). It has

been created by a designer ¹ in 1998 in a brass structure. It is composed of 4 DC motors for the 4 following displacements.

- A motor for the platform rotation (motor 4).
- A motor for the vertical motion of the load (motor 2).
- A motor for the vertical motion of the free mobile pulley (motor 3).
- And next, a motor for the horizontal motion of the load via the translation of the free mobile pulley (motor 1).

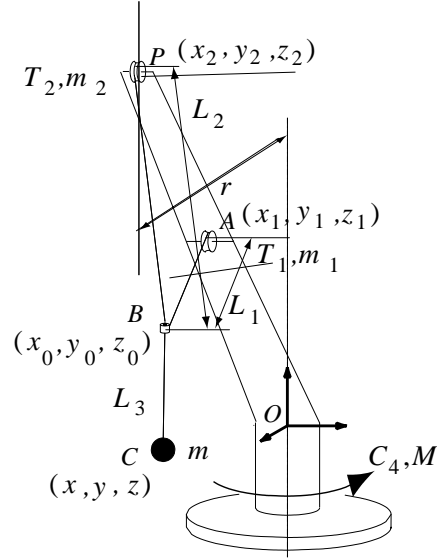


Fig. 2. US Navy crane in 3 dimensions

Sensors of the four motor positions allow to determine the length of the ropes via a correct initialization. Some important coordinates of the crane are used, such as the positions of the fixed pulleys (the coordinates of the pulleys located at A and P are (x_1, y_1, z_1) and (x_2, y_2, z_2)), the coordinates of the load is (x, y, z) (point C) and the position of the mobile pulley is (x_0, y_0, z_0) (point B). Moreover, the three fixed pulleys are lined up and we have $\vec{OA} = \alpha_1 \vec{OP}$.

3. CRANE MODEL

The model of the crane is obtained by Newton's second principle applied to the various rigid bodies constituting the crane (load, motors, free pulley ...). In the model used in this article, the mass of the free pulley is neglected (no dynamics associated to the free pulley). Under this assumption, the load, the free pulley and the ropes BA, BP and CB are in the same plane (Fig. 3(b)). This particular plane's dynamics are described by the angles ξ and φ (Fig. 3(a)), and then, the positions of the ropes and of the load in this plane by the

¹ Walter Rumsey : Artenciel, 24, rue le Regrattier, 75004 Paris, FRANCE. Tel : 01 43 25 73 40, Fax : 01 43 25 73 40

angles γ and β and by the length L_3 . More details are given in (Kiss, 2001)).

First, we introduce three frames. The origin of the first one, denoted by K^b , is fixed at O and its z -axis coincides with the vertical rotation axis of the crane. The two other frames have also their origin at O . The second one, denoted by K^g is chosen such that the z^b -axis of the frame K^b and the point P determine its $x^g z^g$ -plane. These frames are transformed into one another by the rotation of angle ξ around z^b . The last frame, denoted by K is chosen such that the points P , A , and B determine its xz -plane. The transformation between K^g and K is a combination of three rotations of angle α , φ and $-\alpha$ (α is the angle between the jib of the crane and the vertical rotation axis of the crane).

The coordinates of the point C in the frame K are thus obtained as functions of the angles γ and β and the length L_3 (see Fig. 3(b)). Denoting by x_K , y_K and z_K the coordinates of the load in the frame K , we have the following (non differential) equations:

$$\begin{cases} x_K = k \sin \alpha + L_1 \sin(\gamma + (\alpha - \beta)) \\ \quad + L_3 \sin(2\gamma + (\alpha - \beta)) \\ y_K = 0 \\ z_K = k \cos \alpha + L_1 \cos(\gamma + (\alpha - \beta)) \\ \quad + L_3 \cos(2\gamma + (\alpha - \beta)) \end{cases} \quad (1)$$

with L_1 function of β and γ :

$$L_1 = l \frac{\sin \beta}{\sin \gamma}. \quad (2)$$

Note that we also have

$$L_2 = l \frac{\sin(\gamma - \beta)}{\sin \gamma}. \quad (3)$$

Denoting by x_{K^b} , y_{K^b} and z_{K^b} the coordinates of the point C in the frame K^b , the second principle applied to the load reads:

$$m \begin{bmatrix} \ddot{x}_{K^b} \\ \ddot{y}_{K^b} \\ \ddot{z}_{K^b} + g \end{bmatrix} = \Omega_{K^b K^g} \cdot \Omega_{K^g K} \begin{bmatrix} -T_3 \sin \theta \\ 0 \\ T_3 \cos \theta \end{bmatrix} \quad (4)$$

with θ the angle between \overrightarrow{BC} and the z -axis of the frame K , and T_3 the rope tension modulus at C . Finally, the torque balance at A , P and O is given by

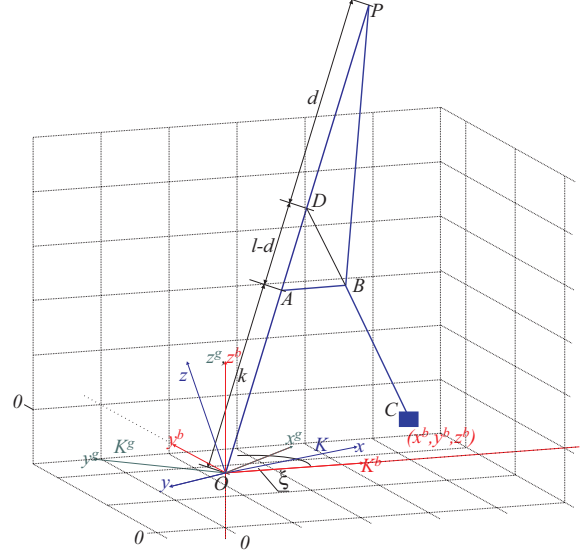
$$\frac{J_1}{\rho_1} \ddot{L}_1 = T_1 \rho_1 - u_1$$

$$\frac{J_2}{\rho_2} \ddot{L} = T_2 \rho_2 - u_2$$

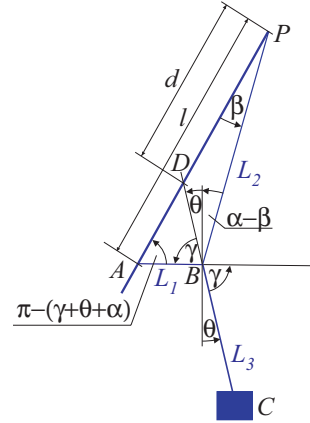
$$J_{pf} \ddot{\xi} = \text{proj}_{z^b} \left(T_2 \left(\overrightarrow{OP} \times \frac{\overrightarrow{PB}}{\|\overrightarrow{PB}\|} \right) + T_1 \left(\overrightarrow{OA} \times \frac{\overrightarrow{AB}}{\|\overrightarrow{AB}\|} \right) \right) + u_4 \quad (5)$$

with $L = L_2 + L_3$, T_1 and T_2 the respective rope tension moduli at the points A and P , u_1 and u_2 the torques delivered by the motors related to the pulleys at A and P , u_4 the torque applied to the platform and J_1 , J_2 and J_{pf} the respective inertias of the motors reported to the points A , P and O .

We can eliminate all the variables but ξ , φ , γ , β , L_3 and their derivatives by combining these equations, to obtain a model of the form $A(X, u)\dot{X} = b(X, u)$ (see (Kiss, 2001) for more details). We then invert $A(X, u)$, to obtain the (nonlinear) explicit form $\dot{X} = f(X, u)$. The measured signal is the vector $Y = (\xi, L_1, L, x_{K^b}, y_{K^b}, z_{K^b})$. The state vector X of dimension 10, is made up with the angles ξ , φ , γ and β , the length L_3 and their first derivatives.



(a) Crane in 3D



(b) Geometry of the crane in 2D

Fig. 3. Geometry of the crane

4. DIFFERENTIAL FLATNESS

The US Navy crane, as for more general cranes, is a differentially flat system. A flat output is remarkably the position of the load ((Kiss, 2001)). So, if we know the position of the load and its derivatives up to the fourth order, we are able to compute the open loop controls that generate the desired trajectory. The proof can be found in (Kiss, 2001).

First, the flatness property is used to generate a rest-to-rest trajectory corresponding to an idle-to-idle displacement of the load. The trajectory, allowing to avoid obstacles, is obtained using polynomial interpolation. In the present case, since we have 10 conditions (5 at the initial point: $x_i, \dot{x}_i, \ddot{x}_i, x_i^{(3)}, x_i^{(4)}$ and 5 at the end: $x_f, \dot{x}_f, \ddot{x}_f, x_f^{(3)}, x_f^{(4)}$), we construct a 9-th degree polynomial for the three coordinates of the load, which reads, for the x coordinate of the load:

$$x(t) = x_i + (x_f - x_i) \left(\frac{t - t_i}{t_f - t_i} \right)^5 \sum_{j=0}^4 a_j \left(\frac{t - t_i}{t_f - t_i} \right)^j \quad (6)$$

with $a_0 = 126$, $a_1 = -420$, $a_2 = 540$, $a_3 = -315$ and $a_4 = 70$.

The same formula is obtained for $y(t)$ and $z(t)$.

From these trajectories, all the system variables can be deduced. In particular, the reference controls of u_1, \dots, u_4 that exactly generate the above trajectories, assuming the exactness of the model and without perturbations, can be deduced ((Fliess *et al.*, 1995; Fliess *et al.*, 1999; Kiss *et al.*, 1999; Kiss *et al.*, 2000a)). The corresponding lengthy formulas are omitted.

5. PD FEEDBACK

We know from (Kiss, 2001) that around any rest-to-rest reference trajectory $(L_{1ref}, L_{ref}, \xi_{ref})$ and $(u_{1ref}, u_{2ref}, u_{4ref})$ of for (L_1, L, ξ) and (u_1, u_2, u_4) respectively, obtained from the previous section, the system is locally stabilized by the following PD controller:

$$\begin{cases} u_1 = u_{1ref} + K_{p1}(L_1 - L_{1ref}) + K_{d1}(\dot{L}_1 - \dot{L}_{1ref}) \\ u_2 = u_{2ref} + K_{p2}(L - L_{ref}) + K_{d2}(\dot{L} - \dot{L}_{ref}) \\ u_4 = u_{4ref} + K_{p4}(\xi - \xi_{ref}) + K_{d4}(\dot{\xi} - \dot{\xi}_{ref}) \end{cases} \quad (7)$$

with the gains K_{p1} , K_{d1} , K_{p2} , K_{d2} , K_{p4} and K_{d4} all positive.

Moreover, this controller makes the end point a globally stable equilibrium.

As announced in the introduction, the tuning of these gains may be quite delicate, depending on the perturbations (frictions, belt elasticity, ...), the parametric errors (on masses, inertias, ...) and the time constants of the displacements. Therefore, to alleviate the duty of this controller, we propose to update the reference trajectory each time the pursuit error exceeds a given bound, the gains of the controller (7) being fixed once for all. However, since the current state from which the new reference trajectory must start is not measured, we need to construct an observer to deduce it from the available measurements. This is the purpose of the next section.

6. OBSERVER

The rope lengths L_1 and $L = L_2 + L_3$, the angle ξ and the coordinates of the load (x , y and z) are measured by two synchronized digital cameras but their successive derivatives have to be estimated. We propose an extended Kalman filter to estimate the vector $(x, \dot{x}, \ddot{x}, x^{(3)}, x^{(4)}, y, \dots, y^{(4)}, z, \dots, z^{(4)})$, which, according to section 4, is necessary to compute all the system state.

Recall that we have denoted by $X = (\xi, \varphi, \gamma, \beta, L_3, \dot{\xi}, \dot{\varphi}, \dot{\gamma}, \dot{\beta}, \dot{L}_3)$ the state vector of the system and that the crane is represented by:

$$\begin{cases} \dot{X} = f(X, u) \\ Y = h(X) \end{cases} \quad (8)$$

with the measurements $Y = (\xi, L_1, L, x, y, z)$.

Its linear tangent approximation along the above trajectory is easily deduced and gives the matrices $A_{lin}(t) = \frac{\partial f}{\partial X}(X_{ref}(t), u_{ref}(t))$, $B_{lin}(t) = \frac{\partial f}{\partial u}(X_{ref}(t), u_{ref}(t))$ and $C_{lin}(t) = \frac{\partial h}{\partial X}(X_{ref}(t))$. The observer has the form

$$\begin{cases} \delta \dot{\hat{X}} = A_{lin}(t)\delta \hat{X} + B_{lin}(t)\delta u + K(Y - \hat{Y}) \\ \hat{Y} = h(\hat{X}) \end{cases} \quad (9)$$

with $\delta \hat{X} = \hat{X} - X_{ref}$. We then calculate the asymptotic gain K of the Kalman filter as a function of the dynamical and observation noise covariance matrices, that are tuned to obtain a fast enough convergence.

Once the state vector \hat{X} of the system is estimated, we obtain the successive derivatives of the flat output by the change of coordinates that maps $\hat{X} = (\hat{\xi}, \hat{\varphi}, \hat{\gamma}, \hat{\beta}, \hat{L}_3, \hat{\xi}, \hat{\varphi}, \hat{\gamma}, \hat{\beta}, \hat{L}_3)$ to $(\hat{x}, \dots, \hat{x}^{(4)}, \hat{y}, \dots, \hat{y}^{(4)}, \hat{z}, \dots, \hat{z}^{(4)})$.

The formulas of this change of coordinates are omitted for simplicity's sake.

To illustrate the results obtained with the above extended Kalman filter, we introduce an output white noise of variance 10^{-6} for the rope lengths, the angle ξ and the coordinates of the load, which corresponds to an average linear deviation of 1 mm and angular deviation of approx. 0.03° , the order of magnitude of the noises on our reduced size setup.

The results are presented in Fig. 4. The observer shows a satisfactory convergence up the 3rd order derivative, and the convergence of the 4th order is still acceptable.

7. PREDICTIVE CONTROL

Define the pursuit error by:

$$e = \sqrt{(\hat{x} - x_{ref})^2 + (\hat{y} - y_{ref})^2} \quad (10)$$

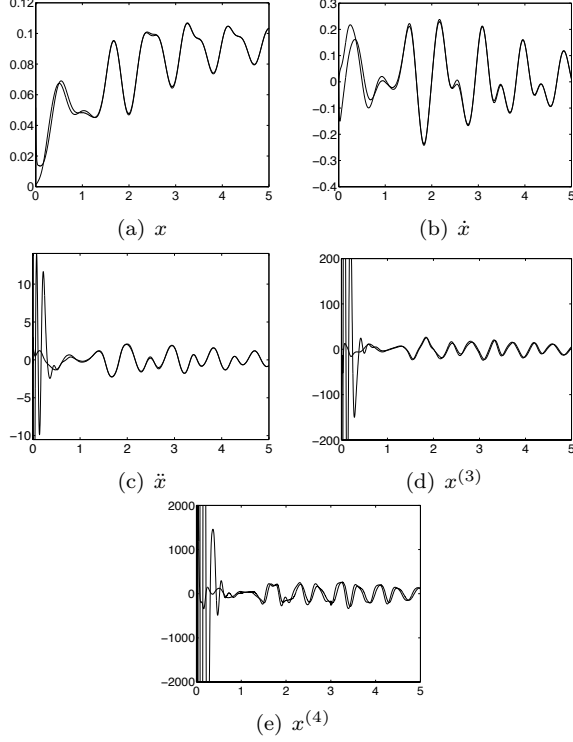


Fig. 4. simulations: Estimated derivatives of the coordinate x with an output noise; (a): x and \hat{x} ; (b): \dot{x} and $\hat{\dot{x}}$; (c): \ddot{x} and $\hat{\ddot{x}}$; (d): $x^{(3)}$ and $\hat{x}^{(3)}$; (e): $x^{(4)}$ and $\hat{x}^{(4)}$.

and let σ be a given positive real number corresponding to the threshold on the error e above which the reference trajectory must be updated. The predictive control algorithm is the following: let \bar{t} be the first time after the initial time t_i such that $e(\bar{t}) = \sigma$. From $\hat{X}(\bar{t})$, computed online, we deduce $\hat{x}(\bar{t}), \dots, \hat{x}^{(4)}(\bar{t}), \hat{y}(\bar{t}), \dots, \hat{y}^{(4)}(\bar{t})$ (z is not considered here since the perturbations acting on it are negligible). Therefore, we can update the reference trajectory starting from the current estimated state at \bar{t} and finishing at rest at a given time $\bar{t} + \tau$, with τ , the receding horizon, to be precised later. Note that the formula (6) is no longer valid since we don't start from a rest point anymore. The new formula is given by:

$$x_{ref}(t) = \hat{x}(\bar{t}) + \sum_{j=1}^9 b_j \left(\frac{t - \bar{t}}{\tau} \right)^j \quad (11)$$

with the b_j 's appropriately computed to arrive at rest at $\bar{t} + \tau$.

The receding horizon τ is chosen according to the following heuristic rule (which can be verified on simulations): the closed-loop input maximal amplitudes remain comparable to the ones of the open-loop references if the horizon τ is of the same order of magnitude as the inverse of the lowest closed-loop eigenfrequency. According to simulations, the frequencies of the response of the closed-loop system with (7) to a perturbation are shown on Fig. 5. Therefore, we choose τ corre-

sponding to an average period. We can verify that it allows to attain the rest point of the load as fast as possible thanks to the reference update (11), without saturating the different motors. Note that this problem is all the more crucial that we want to generate fast motions.

Once the updated trajectory is computed, we check if some inequality constraints on the position, velocity and acceleration of the load are satisfied all along. In case of an affirmative answer, the trajectory y is declared admissible and the corresponding updated reference control is generated. Otherwise, τ is increased.

The same steps apply each time the error happens to increase up to σ .

If the initial state of the trajectory is well estimated, the real motion of the load in response to the updated control fits with the desired trajectory and no oscillations or only small ones remain after $\bar{t} + \tau$.

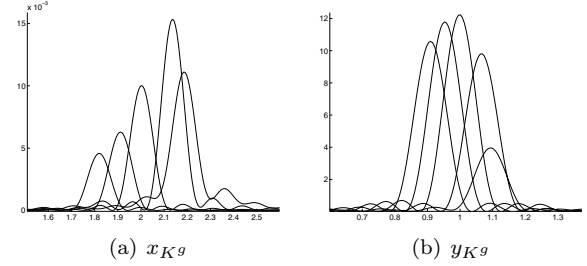


Fig. 5. simulations: Fourier transform of the signals $x(t)$ and $y(t)$ in the frame K^g for different z : $z = 0, 0.25, 0.5, 0.75, 0.1$; (a): oscillation frequencies of x_{K^g} ; (b): oscillation frequencies of y_{K^g} ;

Fig. 6 illustrates our predictive control performances. In this simulation, the coordinates of the load (x, y, z) are sampled at the frequency of 10 Hz, whereas the frequency of the sampled measurements sent by the motor sensors (L, L_1 and the angle ξ) and is about 200 Hz. Moreover, the measurements are corrupted by a bounded noise in the interval $[-10^{-3}, 10^{-3}]$.

An external perturbation is applied to the load at the beginning, at $t = 4$ s and $t = 8$ s, inducing oscillations of an amplitude of about 4 cm on the x and y axis. Piecewise constant voltage perturbations are also applied to the motors. Finally, a real load mass 25 % higher than the one considered in the model is used. The receding horizon of the updated trajectory is $\tau = 0.8$ s. The coordinates of the load and the corresponding motor voltages are presented in the subfigures (d), (e) and (f). It may be seen that the load oscillations and the perturbations on the motors are satisfactorily attenuated thanks to the updated trajectories and the PD corrector.

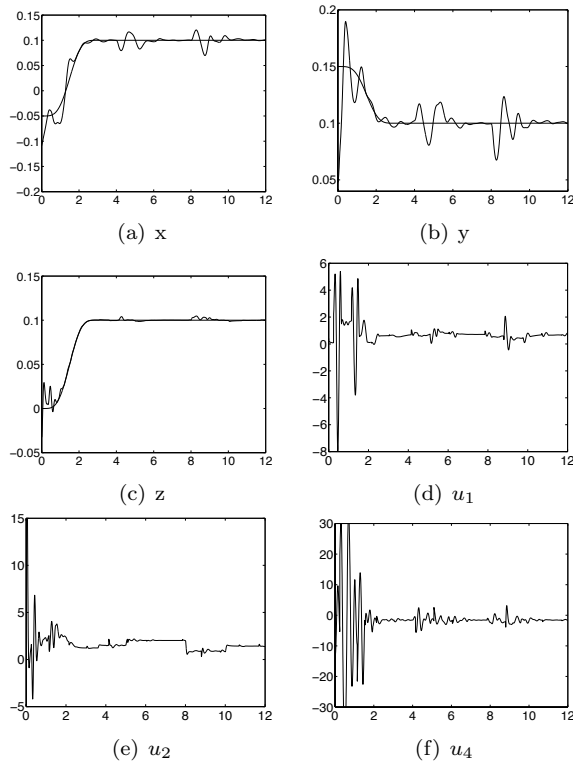


Fig. 6. simulations: Predictive control; (a) Coordinate x real and reference ; (b) Coordinate y real and reference ; (c) Coordinate z real and reference ; (d) Voltage corresponding to the controlled torque u_1 ; (e) Voltage corresponding to the controlled torque u_2 ; (f) Voltage corresponding to the controlled torque u_4 ;

8. CONCLUSION

A flatness-based predictive control to reduce the load oscillations of a reduced size crane has been presented. Simulation results show that this method works as expected. This work is a first step towards its implementation on the crane and further studies, in particular concerning the robustness of this approach, will be done in the near future.

REFERENCES

- Delaleau, E. and V. Hagenmeyer (2006). Commande prédictive non linéaire fondée sur la platitude différentielle. In: *La commande prédictive : Avancées et perspectives* (D. Dumur, Ed.). Hermès. Paris. (33 pages, à paraître).
- Fliess, M. and R. Marquez (2000). Continuous-time linear predictive control and flatness : a module-theoretic setting with examples. *International Journal of Control* **73**, 606–623.
- Fliess, M., J. Lévine, Ph. Martin and P. Rouchon (1995). Flatness and defect of nonlinear systems: introductory theory and examples. *International Journal of Control* **61**(6), 1327–1361.

- Fliess, M., J. Lévine, Ph. Martin and P. Rouchon (1999). A Lie-Bäcklund approach to equivalence and flatness of nonlinear systems. *IEEE Transactions on Automatic Control* **38**, 700–716.
- Kiss, B. (2001). Planification de trajectoires et commande d’une classe de systèmes mécaniques plats et liouvilliens. Thèse École Nationale Supérieure des Mines de Paris.
- Kiss, B., J. Lévine and Ph. Mullhaupt (1999). Modelling, flatness and simulation of a class of cranes. *Periodica Polytechnica* **43**, 215–225.
- Kiss, B., J. Lévine and Ph. Mullhaupt (2000a). Modelling and motion planning for a class of weight handling equipment. *Journal of System Science*.
- Kiss, B., J. Lévine and Ph. Mullhaupt (2000b). A simple output feedback pd controller for non linear cranes. In: *Proceedings of the 39th Conference on Decision and Control*. Sydney, Australia.
- Morari, M. and J.H. Lee (1999). Model predictive control: past, present and future. *Computers & Chemical Engineering* **23**, 667–682.
- Qin, S.J. and T.A. Badwell (2000). An overview of nonlinear model predictive control applications. In: *Nonlinear Predictive Control* (F. Allgöwer and A. Zheng, Eds.). Birkhäuser. Basel. pp. 370–392.